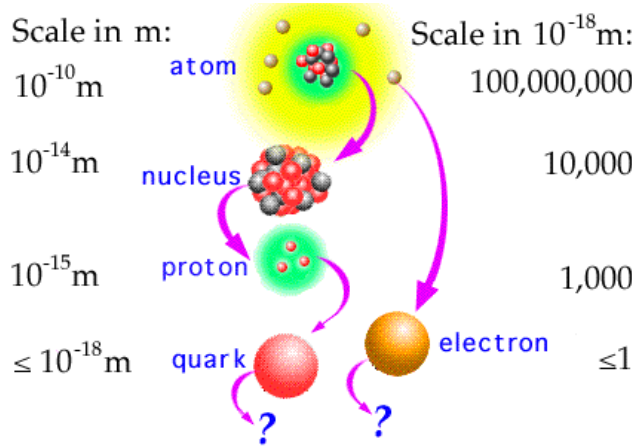


# Electric, Magnetic and Axial Form Factors from Lattice QCD

Rajan Gupta

Theoretical Division

Los Alamos National Laboratory, USA

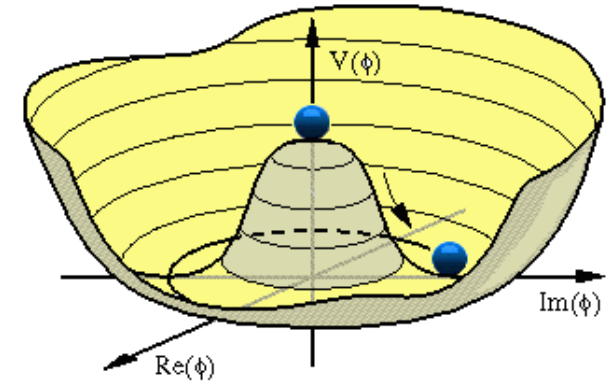


**Elementary Particles**

Quarks			Force Carriers	
$u$ up	$c$ charm	$t$ top	$\gamma$ photon	
$d$ down	$s$ strange	$b$ bottom	$g$ gluon	
$\nu_e$ electron neutrino	$\nu_\mu$ muon neutrino	$\nu_\tau$ tau neutrino	$Z$ Z boson	
$e$ electron	$\mu$ muon	$\tau$ tau	$W$ W boson	

I      II      III

Three Families of Matter



# PNDME Collab.

## clover-on-HISQ

- Tanmoy Bhattacharya
- Vincenzo Cirigliano
- Yong-Chull Jang
- Huey-Wen Lin
- Sungwoo Park
- Boram Yoon

Gupta et al, PRD96 (2017) 114503

Gupta et al, PRD98 (2018) 034503

Lin et al, PRD98 (2018) 094512

Gupta et al, PRD98 (2018) 091501

# NME Collab.

## clover-on-clover

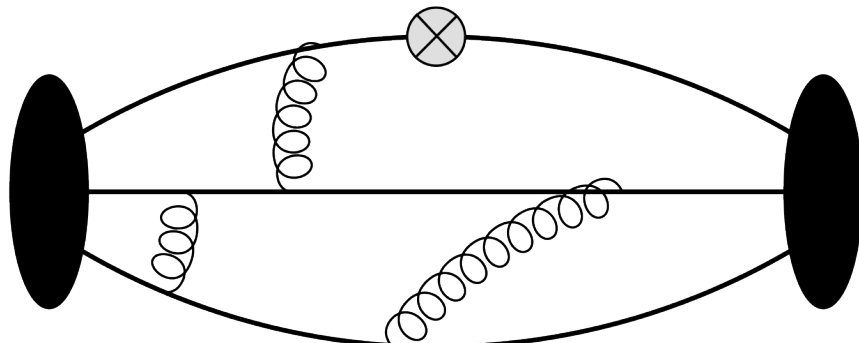
- Tanmoy Bhattacharya
- Vincenzo Cirigliano
- Yong-Chull Jang
- Balint Joo
- Huey-Wen Lin
- Kostas Orginos
- Sungwoo Park
- David Richards
- Frank Winters
- Boram Yoon

# Outline

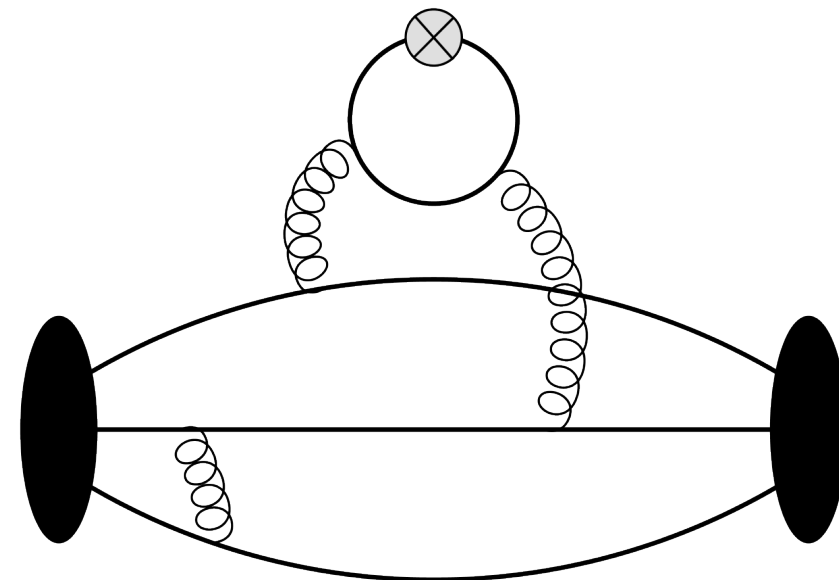
- Physics Motivation
  - Electric and Magnetic form factors extracted from electron and muon scattering
  - Axial vector form factors of nucleon needed for the analysis of neutrino-nucleus scattering:
    - Monitoring neutrino flux
    - Cross-section off various nuclear targets (LAr)
- Challenge: controlling systematic errors in the lattice QCD calculations of the matrix elements of axial and vector current operators within nucleon states

See Community White Paper: arXiv:1904.09931

High precision estimates of the matrix elements of quark bilinear operators within the nucleon state, obtained from “connected” and “disconnected” 3-point correlation functions, needed to address a number of important physics questions



**Connected**



**Disconnected**

# Matrix elements within nucleon states required by many experiments

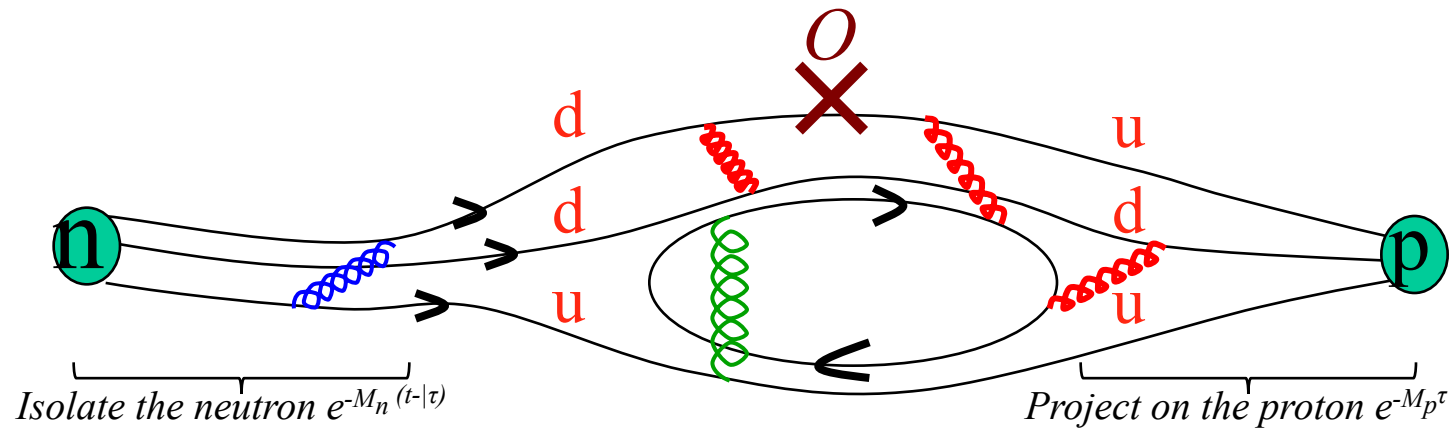
- Isovector charges  $g_A, g_S, g_T$   $\langle p | \bar{u} \Gamma d | n \rangle$
- Axial vector form factors  $\langle p(q) | \bar{u} \gamma_\mu \gamma_5 d(q) | n(0) \rangle$
- Vector form factors  $\langle p(q) | \bar{u} \gamma_\mu d(q) | n(0) \rangle$
- Flavor diagonal matrix elements  $\langle p | \bar{q} q | p \rangle$
- nEDM:  $\Theta$ -term, quark EDM, quark chromo EDM, Weinberg operator, 4-quark operators
- $0\nu\beta\beta$
- Generalized Parton Distribution Functions

# 5 Form Factors

- $G_E(Q^2)$  Electric
- $G_M(Q^2)$  Magnetic
- $G_A(Q^2)$  Axial
- $\tilde{G}_P(Q^2)$  Induced pseudoscalar
- $G_P(Q^2)$  Pseudoscalar
- The lattice methodology is the same
- Precise experimental data exist for  $G_E(Q^2)$  and  $G_M(Q^2)$
- Axial ward identity relates  $G_A(Q^2)$ ,  $\tilde{G}_P(Q^2)$ ,  $G_P(Q^2)$

Lattice QCD has to predict all 5,  $g_A$ ,  $\mu$

# Calculating matrix elements using Lattice QCD



$$\langle \Omega | \hat{N}(t, p') \hat{O}(\tau, p' - p) \hat{N}(0, p) | \Omega \rangle =$$

$$\sum_{i,j} \langle \Omega | \hat{N}(p') | N_j \rangle e^{-\int dt H} \langle N_j | \hat{O}(\tau, p' - p) | N_i \rangle e^{-\int dt H} \langle N_i | \hat{N}(p) | \Omega \rangle =$$

$$\sum_{i,j} \langle \Omega | \hat{N}(p') | N_j \rangle e^{-E_j(t-\tau)} \langle N_j | \hat{O}(\tau, p' - p) | N_i \rangle e^{-E_i\tau} \langle N_i | \hat{N}(p) | \Omega \rangle$$

# Electric & Magnetic form factors

**Matrix Elements of  $V_\mu \rightarrow$  Dirac ( $F_1$ ) and Pauli ( $F_2$ ) form factors**

$$\langle N(p_f) | V^\mu(q) | N(p_i) \rangle = \bar{u}(p_f) \left[ \gamma^\mu F_1(q^2) + \sigma^{\mu\nu} q_\nu \frac{F_2(q^2)}{2M} \right] u(p_i)$$

**Define Sachs Electric ( $G_E$ ) and Magnetic ( $G_M$ ) form factors**

$$G_E(q^2) = F_1(q^2) - \frac{q^2}{4M^2} F_2(q^2), \quad G_M(q^2) = F_1(q^2) + F_2(q^2)$$

# Challenges to obtaining high precision results for matrix elements within nucleon states

- High Statistics:  $O(1,000,000)$  measurements
- Demonstrating control over all Systematic Errors:
  - Contamination from excited states
  - $Q^2$  behavior of form factors
  - Non-perturbative renormalization of bilinear operators ( $RI_{\text{smom}}$  scheme)
    - Finite volume effects
    - Chiral extrapolation to physical  $m_u$  and  $m_d$  (simulate at physical point)
    - Extrapolation to the continuum limit (lattice spacing  $a \rightarrow 0$ )

Perform simulations on ensembles with multiple values of

- Lattice size:  $M_\pi L \rightarrow \infty$
- Light quark masses:  $\rightarrow$  physical  $m_u$  and  $m_d$
- Lattice spacing:  $a \rightarrow 0$

# Analyzing lattice data $\Omega(a, M_\pi, M_\pi L)$ : Simultaneous CCFV fits versus $a, M_\pi^2, M_\pi L$

Include leading order corrections to fit lattice data w.r.t.

- Lattice spacing:  $a$
- Dependence on light quark mass:  $m_q \sim M_\pi^2$
- Finite volume:  $M_\pi L$

$$r^2_A(a, M_\pi, M_\pi L) = c_0 + c_1 a + c_2 M_\pi^2 + c_3 M_\pi^2 e^{-M_\pi L} + \dots$$

# Toolkit

- Multigrid Dirac invertor → propagator  $S_F = D^{-1}\eta$
- Truncated solver method with bias correction (AMA)
- Coherent source sequential propagator
- Deflation + hierarchical probing
- High Statistics
- 3-5 values of  $t_{\text{sep}}$  with smeared sources for  $S_F$
- 2-, 3-, n-state fits to multiple values of  $t_{\text{sep}}$
- Non-perturbative methods for renormalization constants
- Combined extrapolation in  $a$ ,  $M_\pi$ ,  $M_\pi L$  (CCFV)
- Variation of results with CCFV extrapolation Ansatz

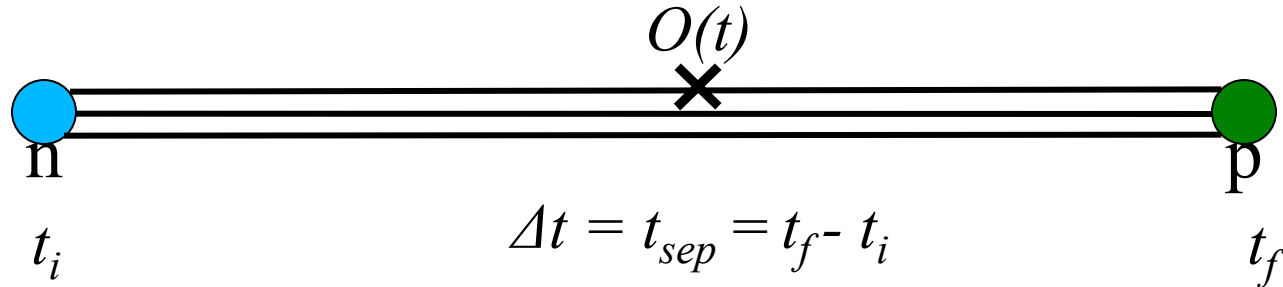
## Controlling excited-state contamination: n-state fit

$$\Gamma^2(t) = |A_0|^2 e^{-M_0 t} + |A_1|^2 e^{-M_1 t} + |A_2|^2 e^{-M_2 t} + |A_3|^2 e^{-M_3 t} + \dots$$

$$\begin{aligned}\Gamma^3(t, \Delta t) = & |A_0|^2 \langle 0 | O | 0 \rangle e^{-M_0 \Delta t} + |A_1|^2 \langle 1 | O | 1 \rangle e^{-M_1 \Delta t} + \\ & A_0 A_1^* \langle 0 | O | 1 \rangle e^{-M_0 \Delta t} e^{-\Delta M (\Delta t - t)} + A_0^* A_1 \langle 1 | O | 0 \rangle e^{-\Delta M t} e^{-M_0 \Delta t} + \dots\end{aligned}$$

$M_0, M_1, \dots$  masses of the ground & excited states

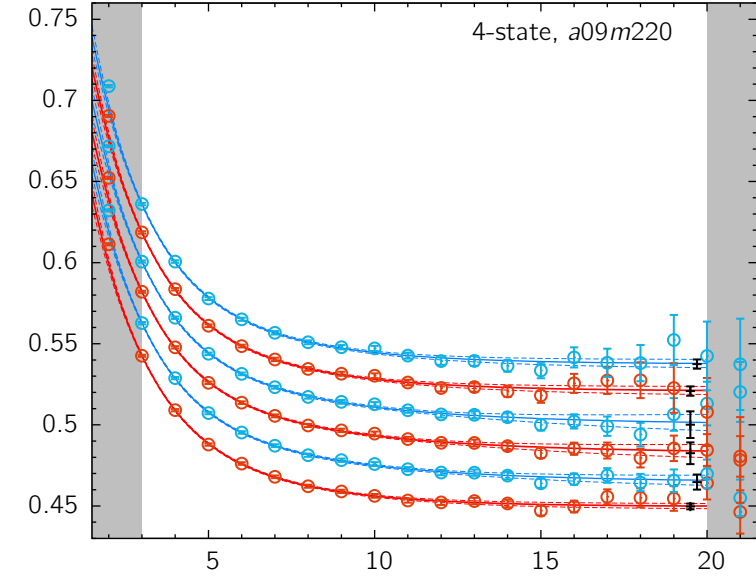
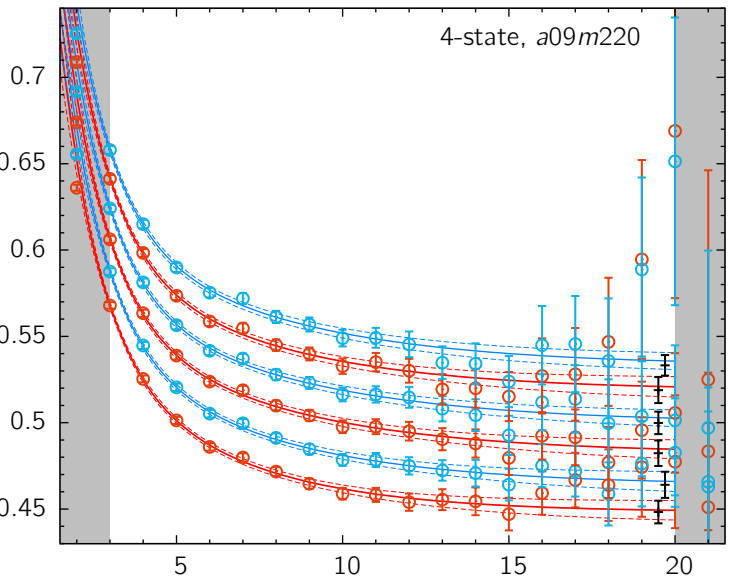
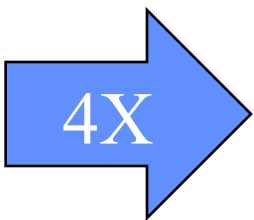
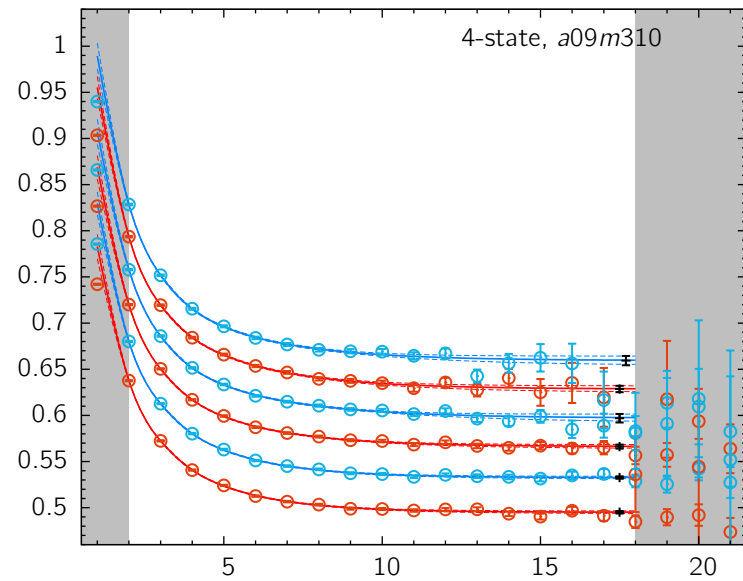
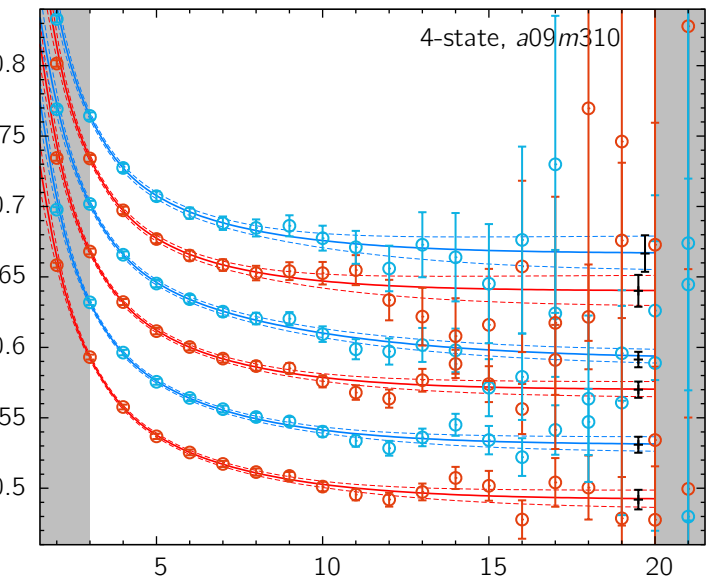
$A_0, A_1, \dots$  corresponding amplitudes



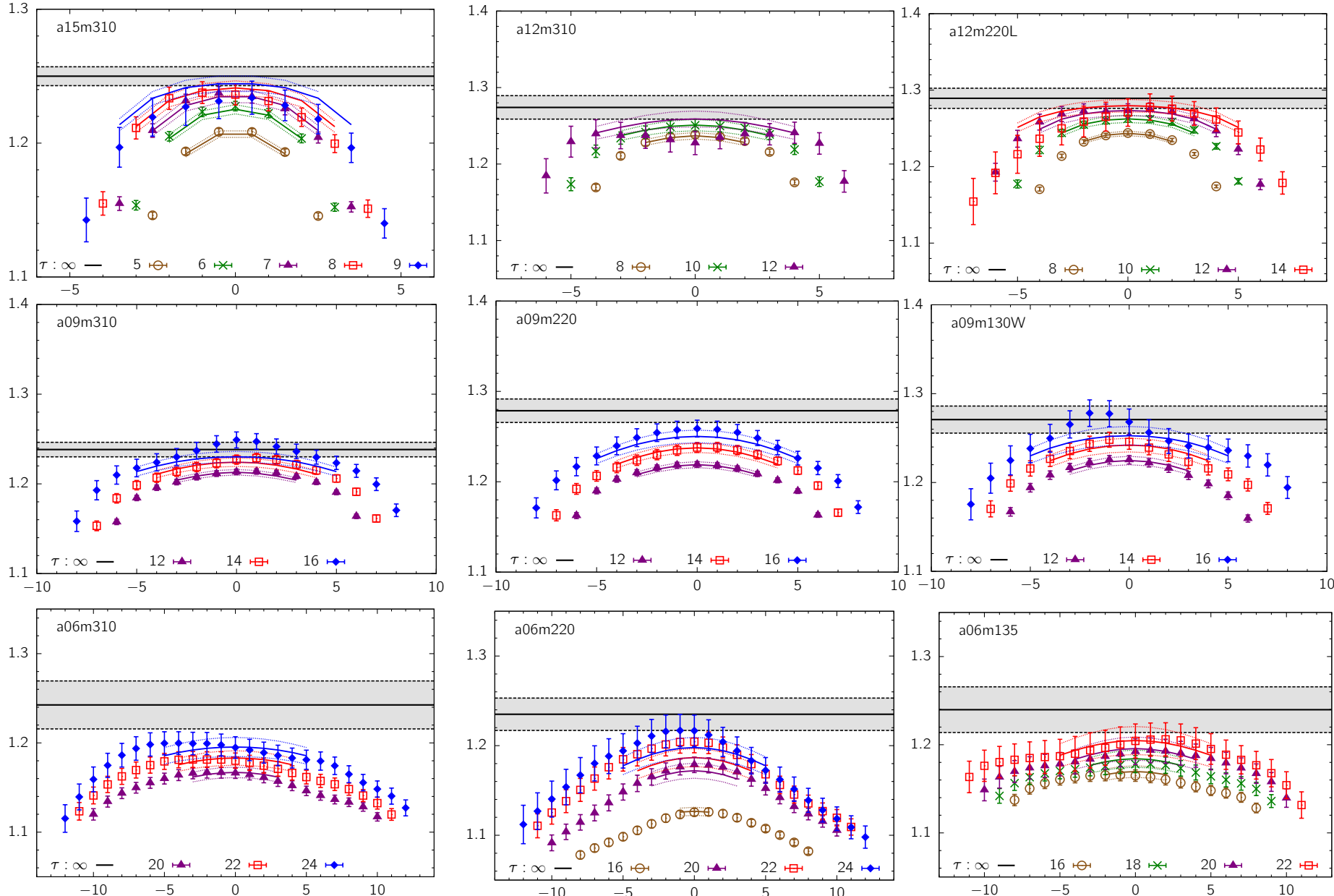
Make a simultaneous fit to data at multiple  $\Delta t = t_{sep} = t_f - t_i$

KEY quantity to control:  $M_1$  (first excited state mass)

# 4-state fit to 2-point correlation function

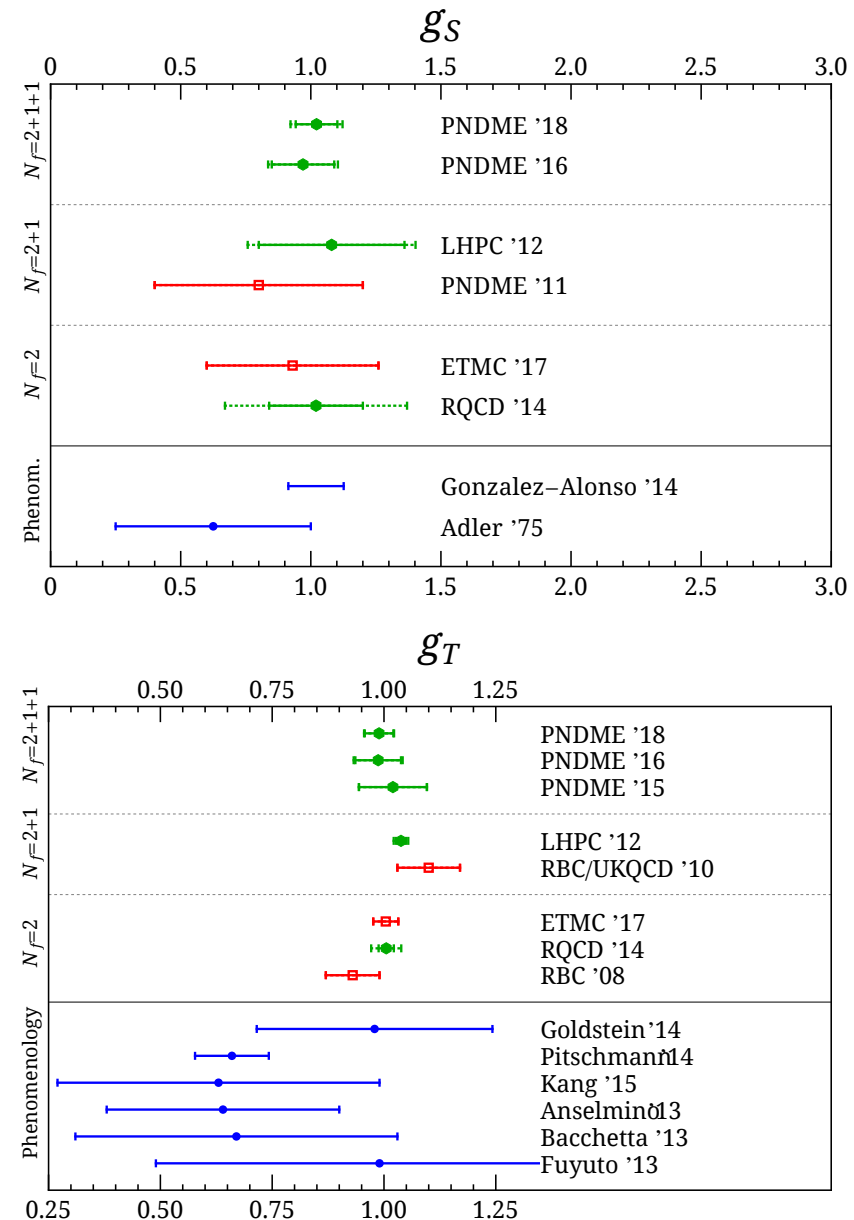
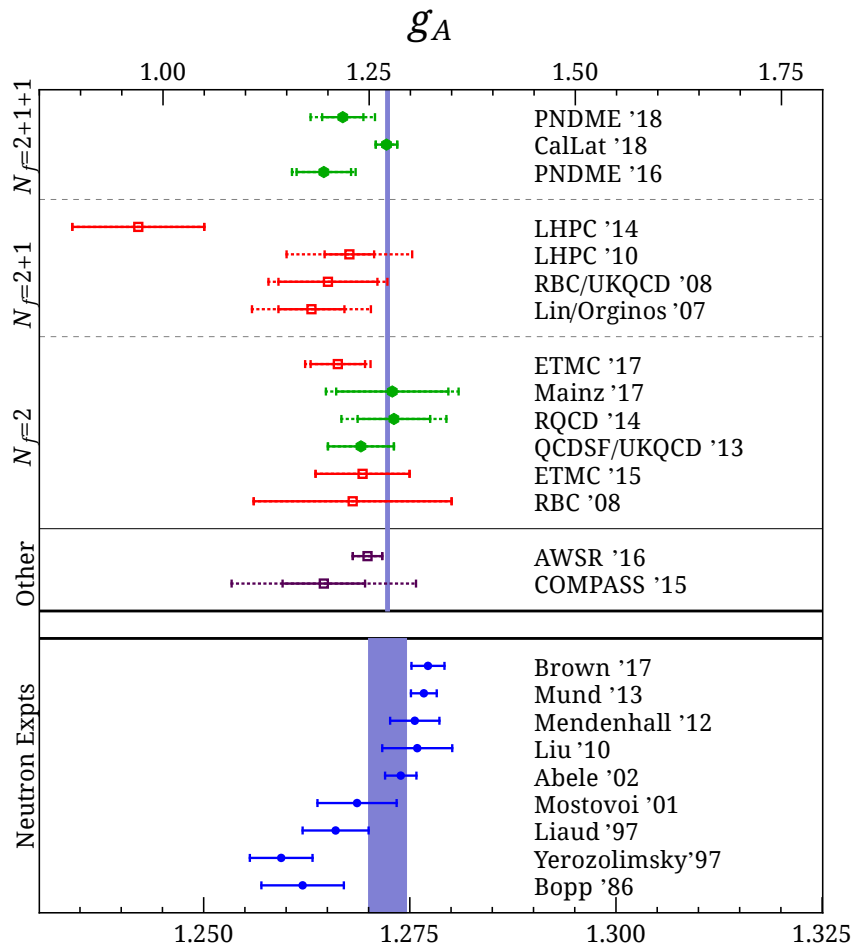


# $g_A$ : Excited State Contamination



Data from 9 clover-on-HISQ ensembles and 3\*-state fits : Gupta et al, PhysRevD.98.034503

# Status 2018: Isovector $g_A$ , $g_S$ , $g_T$



# $g_A^{u-d}$ : PNDME & Callat agree within errors on 7 ensembles

CallLat: Nature: <https://doi.org/10.1038/s41586-018-0161-8>

PNDME: Gupta et al, Phys. Rev. D98 (2018) 034503

	PNDME	CallLat
a15m310	1.228(25)	1.215(12)
a12m310	1.251(19)	1.214(13)
a12m220S	1.224(44)	1.272(28)
a12m220	1.234(25)	1.259(15)
a12m220L	1.262(17)	1.252(21)
a09m310	1.235(15)	1.236(11)
a09m220	1.260(19)	1.253(09)

CallLat uses a variant of the summation method

Difference comes from the Chiral-Continuum fits:

- CallLat chiral fit anchored by heavier pion masses
- CallLat have not yet analyzed the  $a=0.06\text{fm}$  lattices

# Steps in the FF calculations

- Calculate matrix elements for different  $t_{sep}$
- Control excited-state contamination:  $p=0$ ,  $p\neq 0$
- From different Lorentz components & the momentum dependence extract the form factors
- Fit  $Q^2$  behavior of  $G_i(q^2)$ : (dipole, z-expansion, ...)
- Calculate  $r_i(a, M_\pi, M_\pi L)$ :  $\langle r_i^2 \rangle = -\frac{6}{dq^2} \left[ \frac{\hat{G}_i(q^2)}{\hat{G}_i(0)} \right]_{q^2=0}$
- Extrapolate  $r_i$  ( $a \rightarrow 0$ ,  $M_\pi L \rightarrow \infty$ ,  $M_\pi \rightarrow 135\text{MeV}$ )

# Electric & Magnetic form factors

**Matrix Elements of  $V_\mu \rightarrow$  Dirac ( $F_1$ ) and Pauli ( $F_2$ ) form factors**

$$\langle N(p_f) | V^\mu(q) | N(p_i) \rangle = \bar{u}(p_f) \left[ \gamma^\mu F_1(q^2) + \sigma^{\mu\nu} q_\nu \frac{F_2(q^2)}{2M} \right] u(p_i)$$

**Define Sachs Electric ( $G_E$ ) and Magnetic ( $G_M$ ) form factors**

$$G_E(q^2) = F_1(q^2) - \frac{q^2}{4M^2} F_2(q^2), \quad G_M(q^2) = F_1(q^2) + F_2(q^2)$$

# Extracting EM form factors

$$\sqrt{2E_p(M_N + E_p)} \ Re(R_i) = -\epsilon_{ij3} q_j G_M$$

$$\sqrt{2E_p(M_N + E_p)} \ Im(R_i) = q_i G_E$$

$$\sqrt{2E_p(M_N + E_p)} \ Re(R_4) = (M_N + E_p) G_E$$

Each matrix element gives one form factor

ESC in  $\text{Im } (R_i)$  is large

# Experimental Results

$$r_E = 0.875(6) \text{ fm}$$

Electron scattering

$$r_E = 0.8409(4) \text{ fm}$$

Muonic hydrogen

$$r_M = 0.86(3) \text{ fm}$$

$$\mu_P = 2.7928$$

$$\mu_N = -1.9130$$

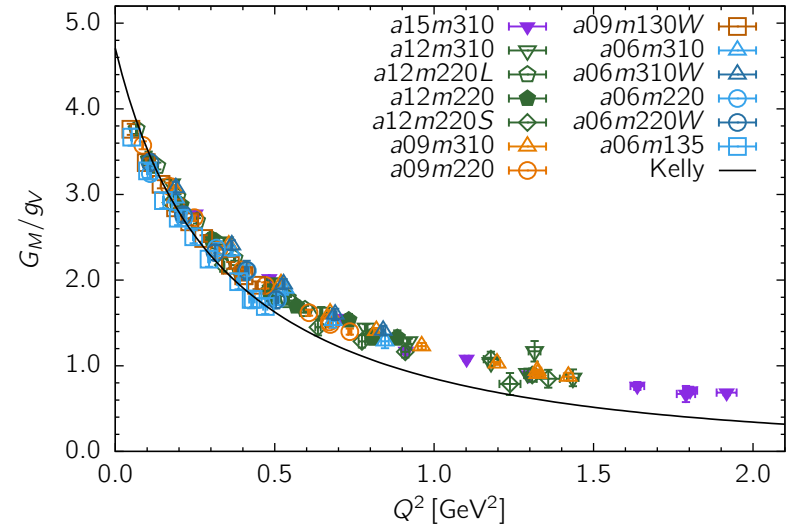
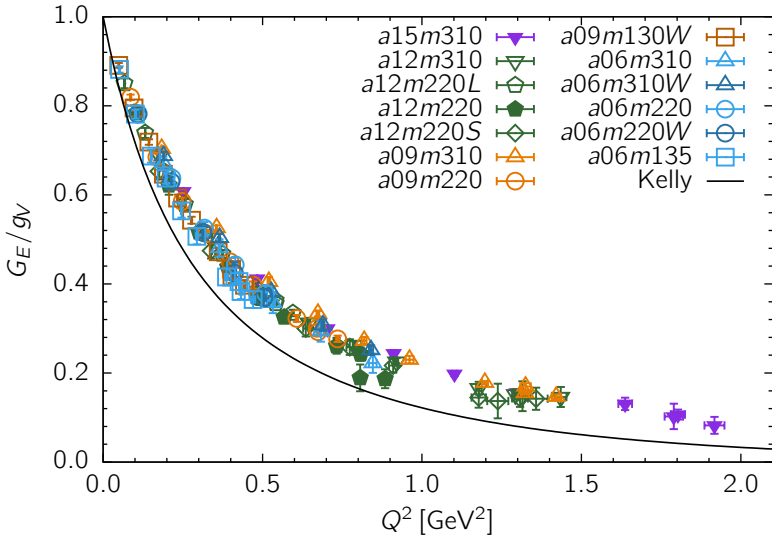
$$r_E^{p-n} = 0.93 \text{ fm}$$

Isovector radii

$$r_M^{p-n} = 0.87 \text{ fm}$$

We will focus on the primary quantities  $G_E(Q^2), G_M(Q^2)$

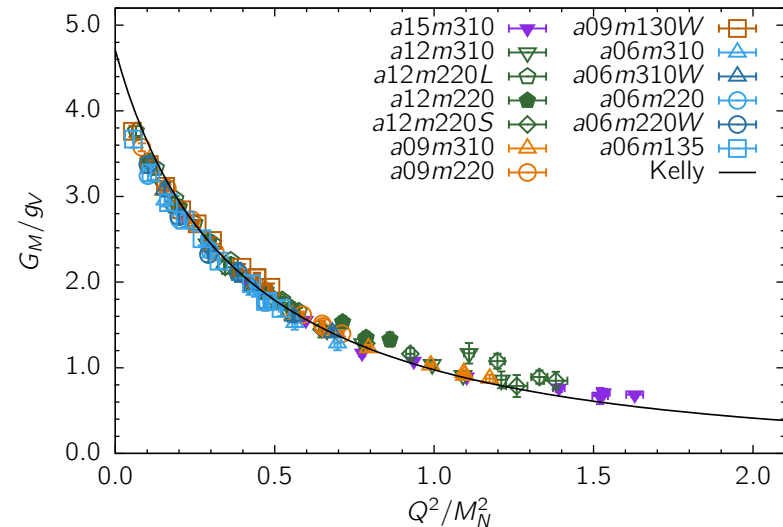
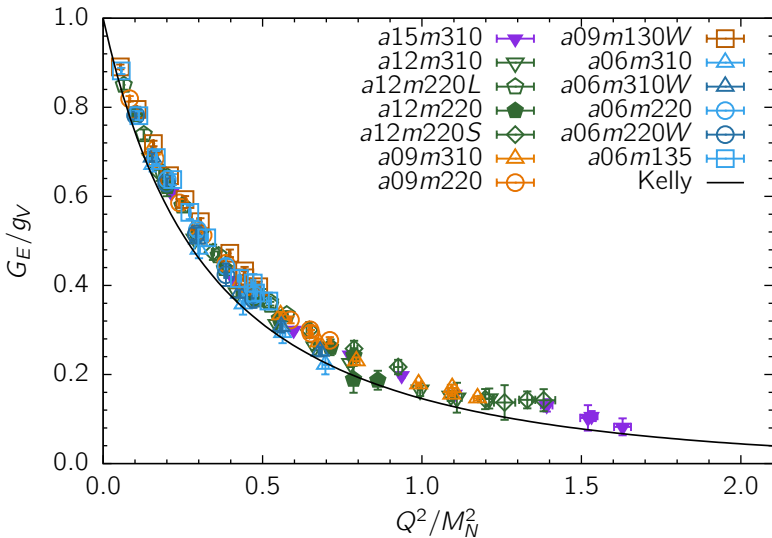
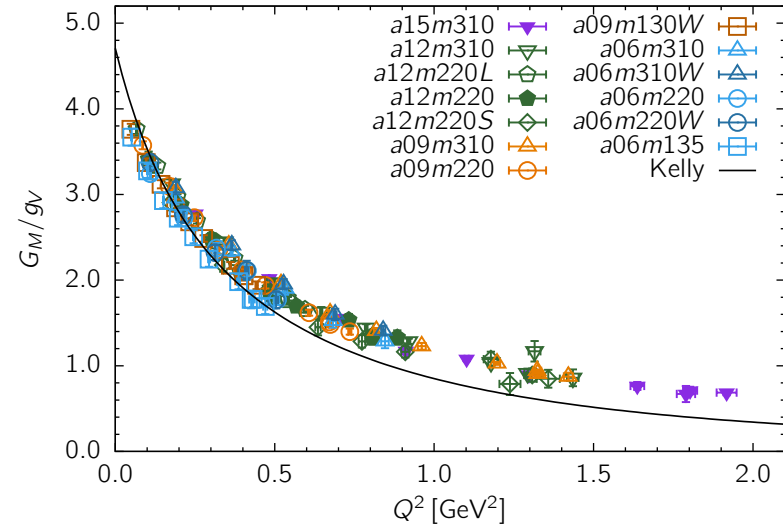
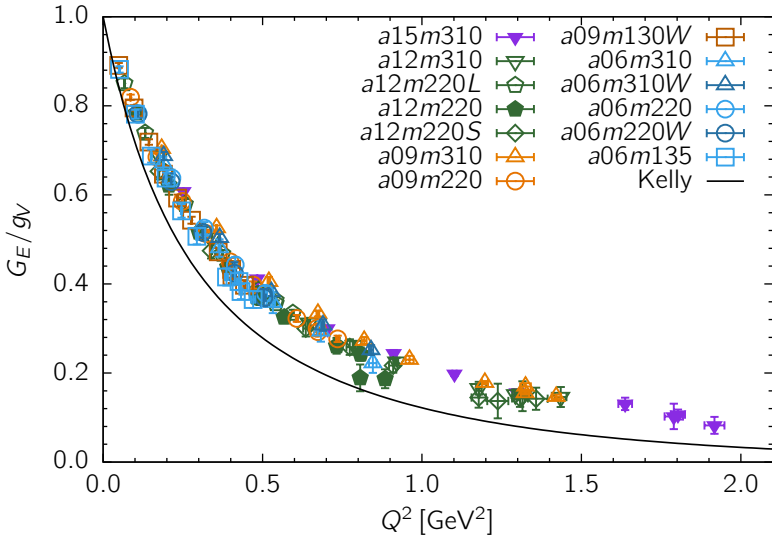
# Clover-on-HISQ data



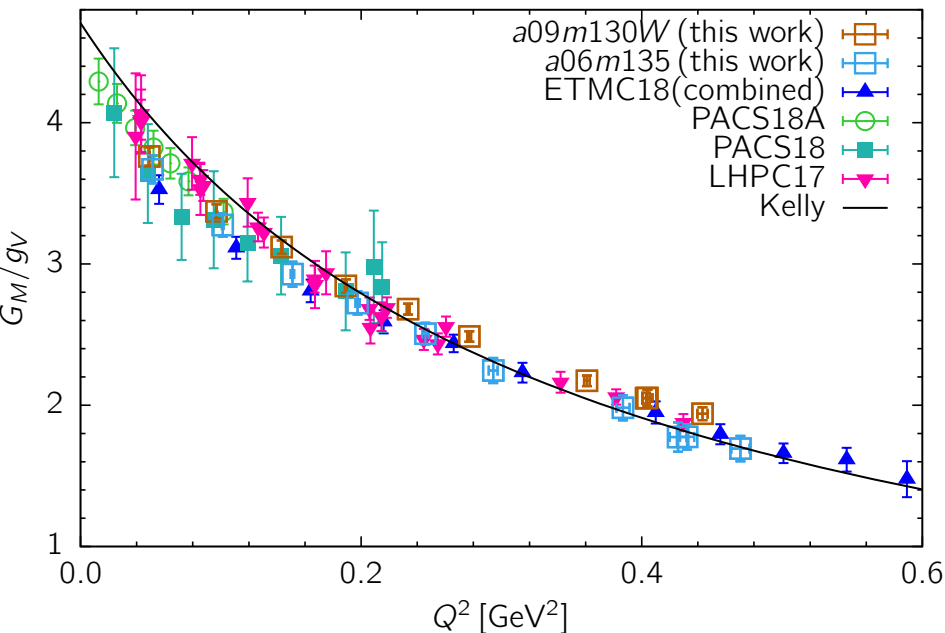
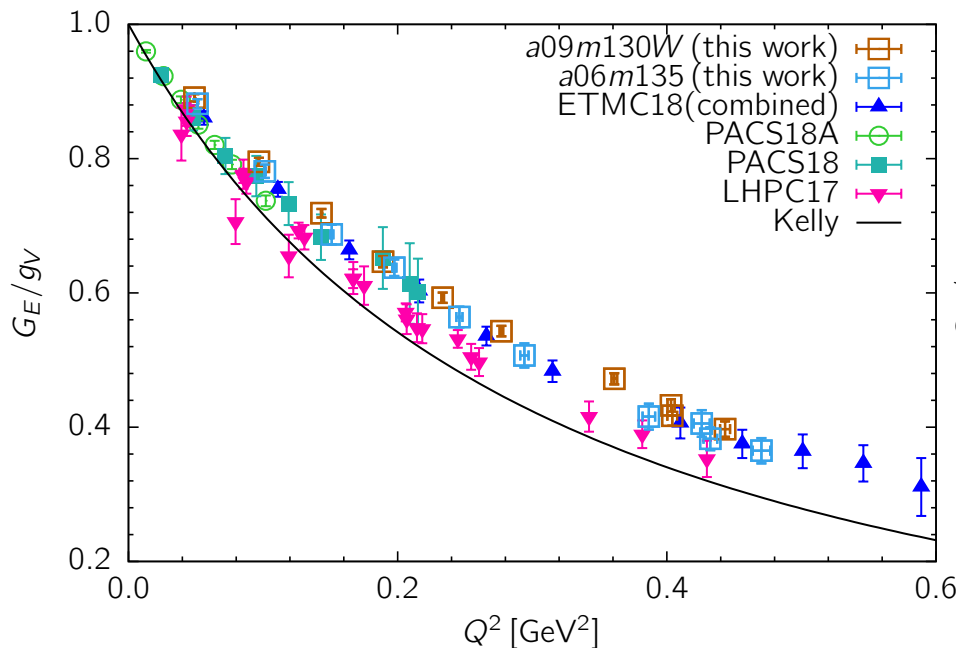
Data collapse into a single curve implies that  $G_E(Q^2)$ ,  $G_M(Q^2)$  are insensitive to the lattice spacing, pion mass, lattice volume

The phenomenological Kelly curve shown for reference.  
It is not the target of lattice calculations!

# Clover-on-HISQ data

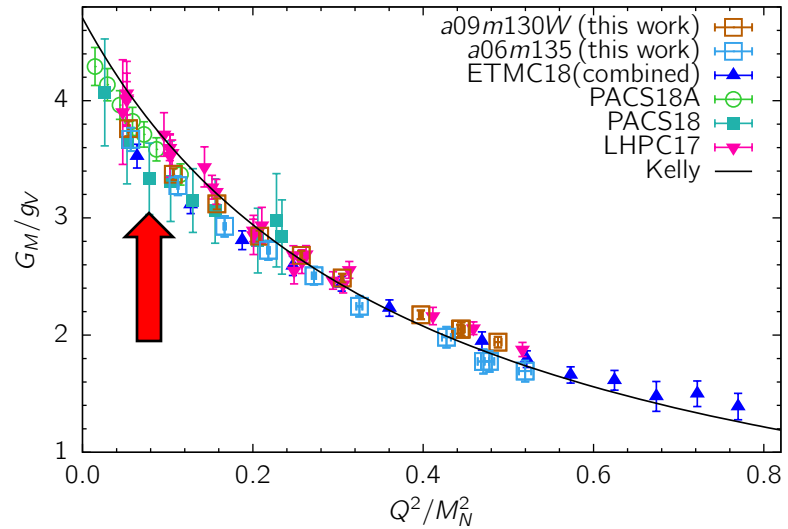
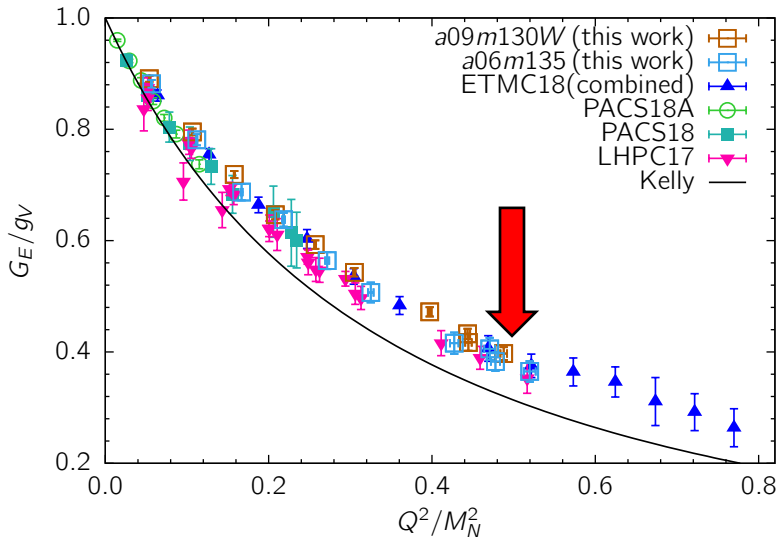
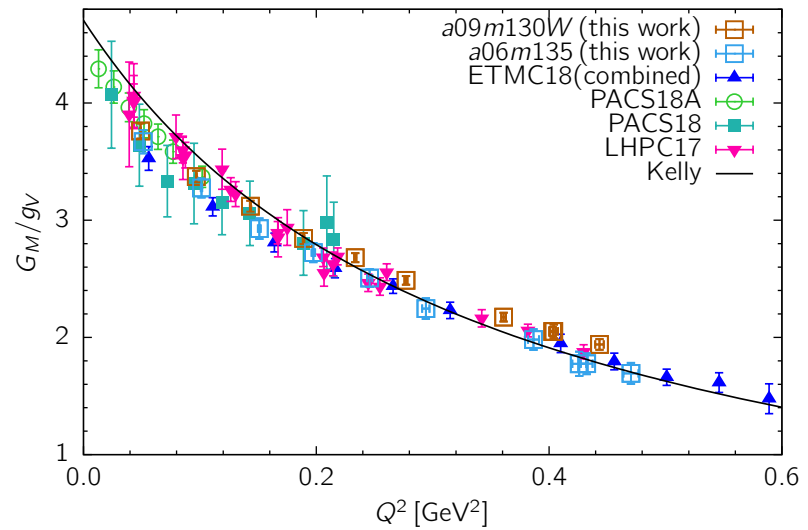
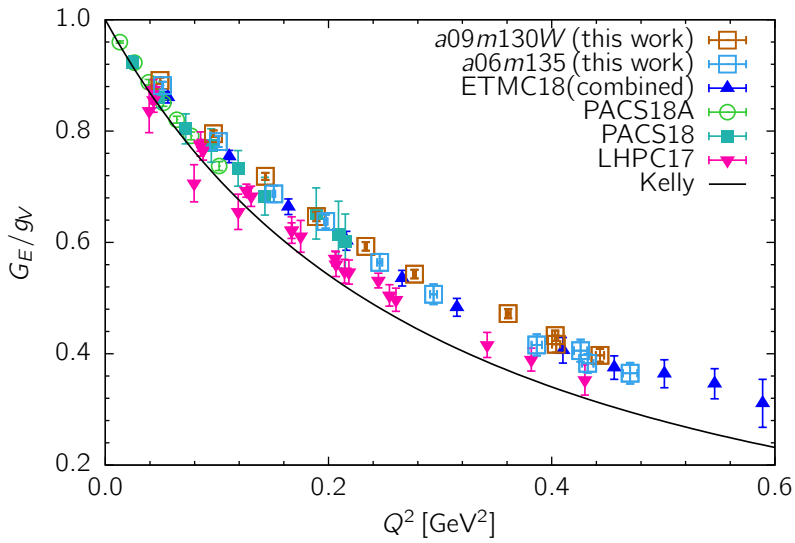


# Comparison of $M_\pi \sim 135\text{MeV}$ data



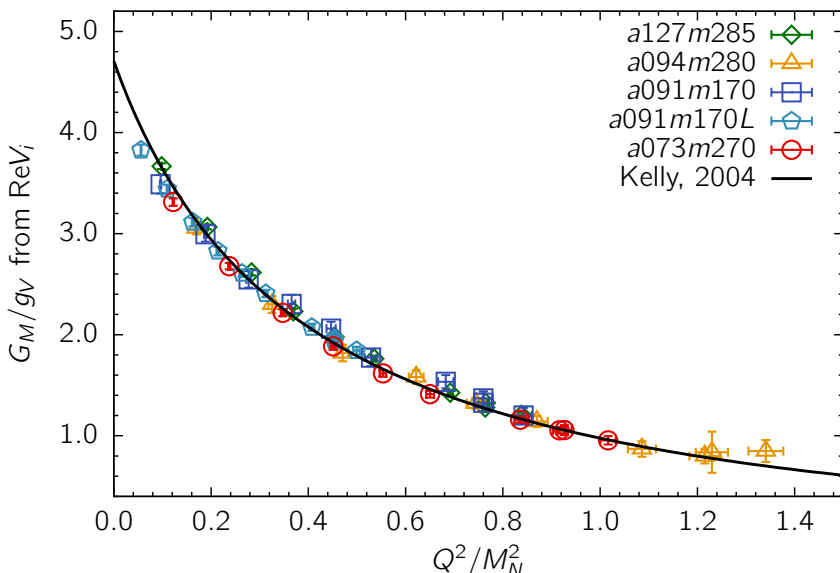
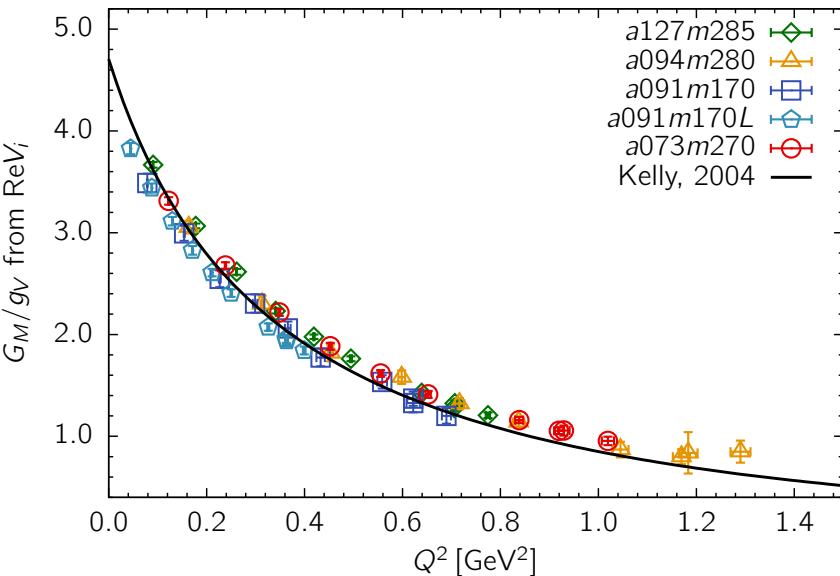
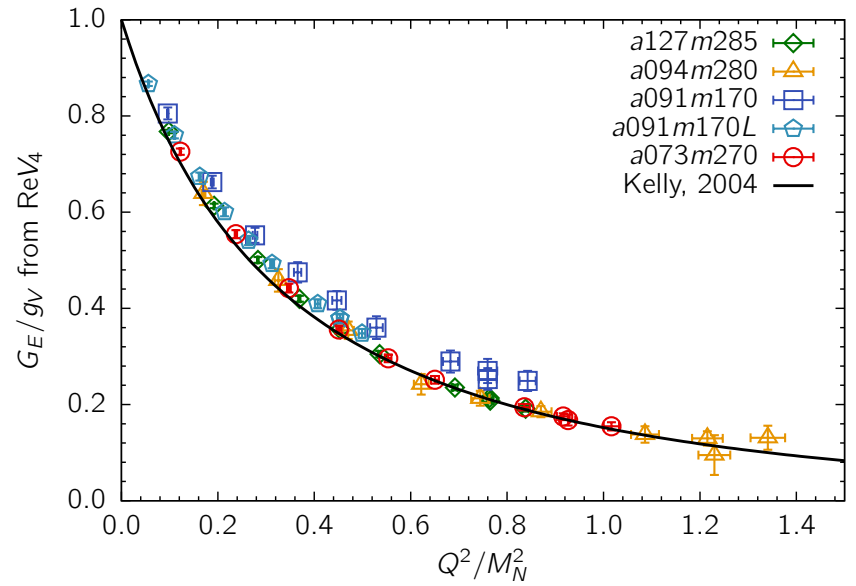
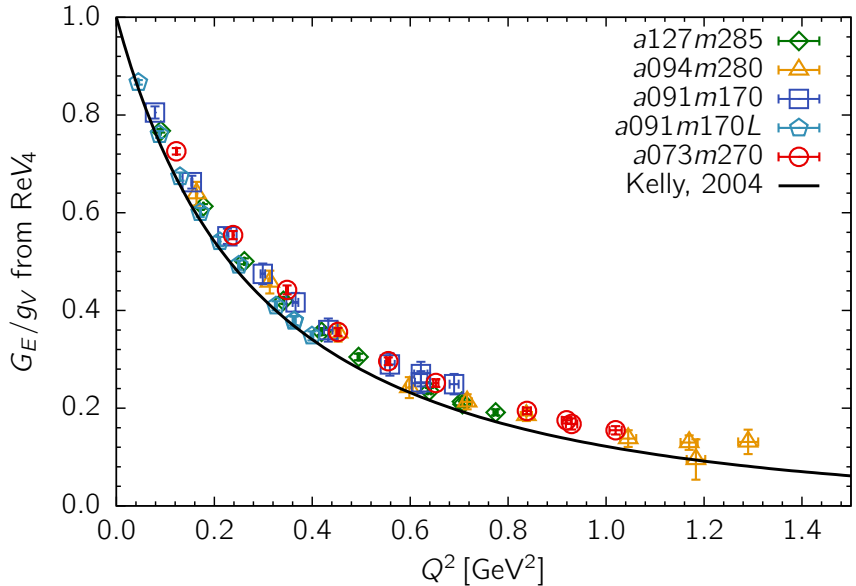
Data from different collaborations collapsing onto a single curve implies that  $G_E(Q^2)$ ,  $G_M(Q^2)$  are also insensitive to the number of flavors: 2, 2+1, 2+1+1

# Comparison of $M_\pi \sim 135\text{MeV}$ data



# Clover-on-clover data

NME unpublished



# Kelly Parameterization

Kelly parameterization of the experimental data for  $G_E$ ,  $G_M$

$$\hat{G}_X(Q^2) = \frac{\hat{G}(0) \sum_{k=0}^n a_k \tau^k}{\left\{ 1 + \sum_{k=1}^{n+2} b_k \tau^k \right\}}, \quad \hat{G}_Y(Q^2) = \frac{A\tau}{1 + B\tau} \frac{1}{\left( 1 + Q^2/0.71\text{GeV}^2 \right)^2}$$

where  $\tau = Q^2/4\mathcal{M}^2$ . The parameters  $\mathcal{M}$ ,  $G(0)$ ,  $a_k$ ,  $b_k$ ,  $A$ , and  $B$  are determined from fit to the data.

Do the "experimental data" have all corrections included?

# z-expansion

The form factors are analytic functions of  $Q^2$  below a cut starting at n-particle threshold  $t_{cut}$ .

A model independent approach is the  $z$ -expansion:

$$\hat{G}(Q^2) = \sum_{k=0}^{\infty} a_k z(Q^2)^k \quad \text{with} \quad z = \frac{\sqrt{t_{cut} + Q^2} - \sqrt{t_{cut} + Q_0^2}}{\sqrt{t_{cut} + Q^2} + \sqrt{t_{cut} + Q_0^2}}$$

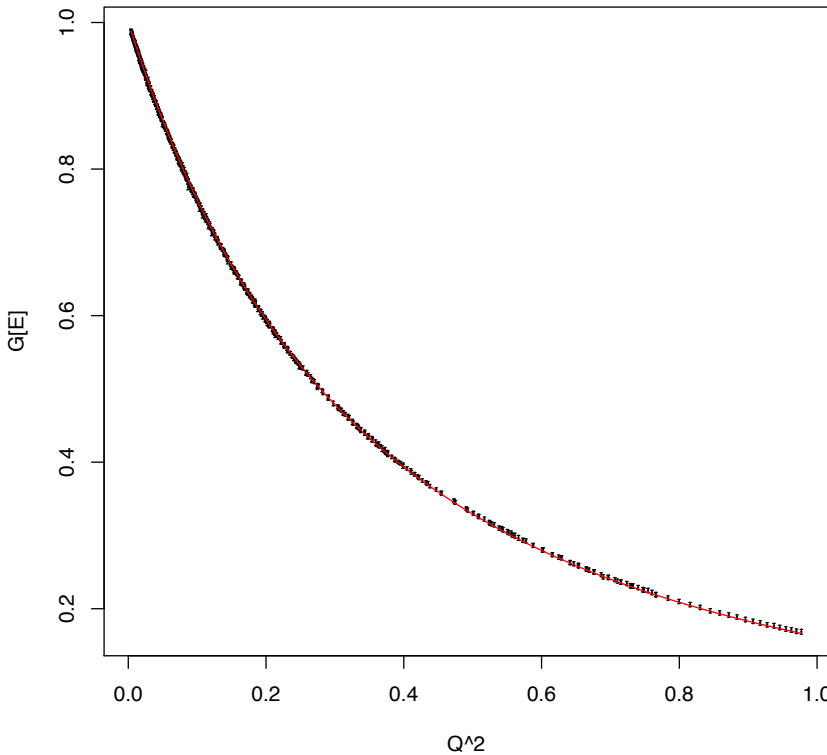
with  $t_{cut} = 4m_\pi^2$  for  $G_{E,M}$  and  $t_{cut} = 9m_\pi^2$  for  $G_A$ . We choose  $Q_0 = 0$

Incorporate  $1/Q^4$  behavior as  $Q^2 \rightarrow \infty$  via sum rules

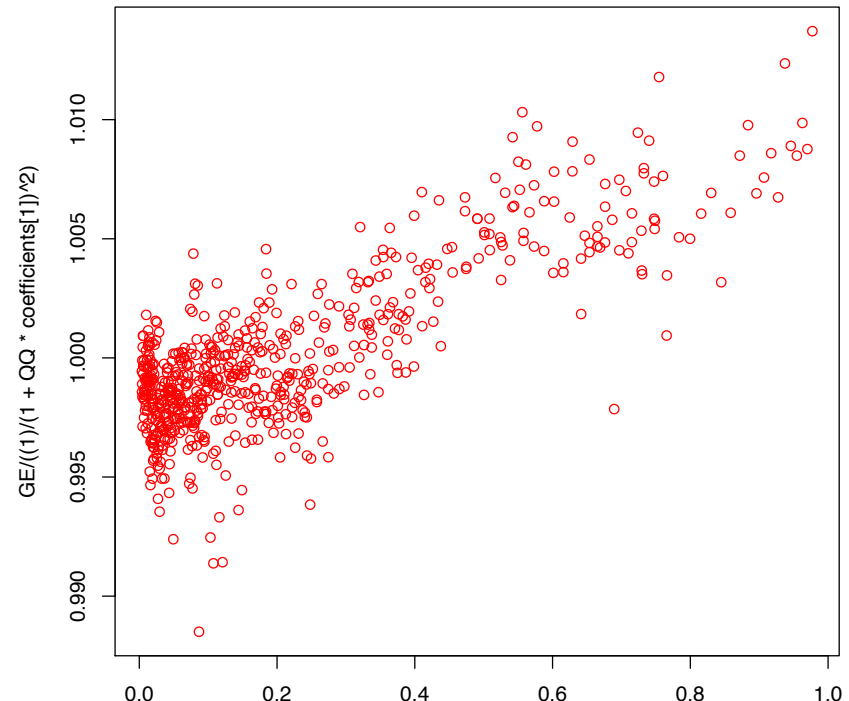
Impose Bound  $|a_k| < 5$

Results independent of truncation for  $k \geq 4$

# Is dipole a good model?



dipole fit to Mainz data for  $G_E$



$\frac{\text{Mainz } G_E \text{ data}}{\text{dipole fit}}$

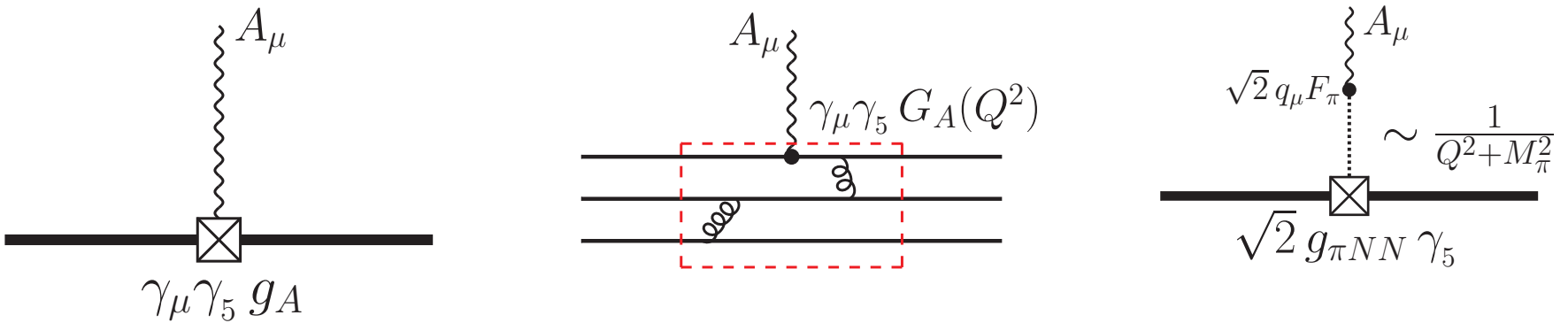
Yes for  $G_E$  ( $\sim 1\%$ ), not so for  $G_M$  ( $\sim 6\%$ )

Thanks to D. Higinbotham for providing his version of the binned Mainz data

# Summary: Electric and Magnetic form factors

- $G_E(Q^2), G_M(Q^2)$  show small variation with  $a$  and  $M_\pi$ : PNDME data (9 clover-on-HISQ ensembles) fall on a single curve
- The curve becomes narrower and closer to the “Kelly curve” when plotted versus  $Q^2/M_N^2$
- World data for  $G_E(Q^2), G_M(Q^2)$  with  $M_\pi \sim 135 MeV$  also collapse to this curve
- Deviations from the “Kelly curve” are within possible errors
  - Excited-state effects large at small  $Q^2$  for  $G_M(Q^2)$
  - Excited-state effects in  $G_E$  small for  $Q^2 \sim 0$ , but increase with  $Q^2$
  - Lattice artifacts increase as  $Q^2$  increases

# Axial-vector form factors



On the lattice we can calculate 3 form factors from ME of  $V_\mu$  and  $A_\mu$ :

- Axial:  $G_A$
- Induced pseudoscalar:  $\tilde{G}_P$
- Pseudoscalar:  $G_P$

$$\langle N(p_f) | A^\mu(q) | N(p_i) \rangle = \bar{u}(p_f) \left[ \gamma^\mu G_A(q^2) + q_\mu \frac{\tilde{G}_P(q^2)}{2M} \right] \gamma_5 u(p_i)$$

$$\langle N(p_f) | P(q) | N(p_i) \rangle = \bar{u}(p_f) G_P(q^2) \gamma_5 u(p_i)$$

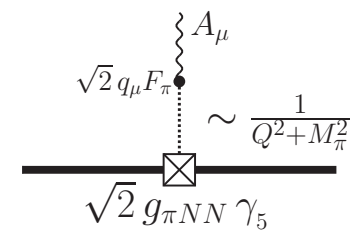
The 3 form factors are related by PCAC  $\partial_\mu A_\mu = 2mP$

PCAC ( $\partial_\mu A_\mu = 2\hat{m}P$ ) requires

$$2\hat{m}G_P(Q^2) = 2M_N G_A(Q^2) - \frac{Q^2}{2M_N} \tilde{G}_P(Q^2)$$

Pion pole-dominance hypothesis

$$\tilde{G}_P(Q^2) = G_A(Q^2) \left[ \frac{4M_N^2}{Q^2 + M_\pi^2} \right]$$



If pion pole-dominance holds  
 $\Rightarrow$  there is only one independent form factor

Goldberger-Treiman relation

$$F_\pi \ g_{\pi NN} = M_N \ g_A$$

## Dipole ansatz for $q^2$ behavior of $G_E$ , $G_M$ , $G_A$

$$G_i(q^2) = \frac{G_i(0)}{\left(1 + \frac{q^2}{M_i^2}\right)^2} \quad M_i \text{ is the dipole mass}$$

- Corresponds to exponential decaying distribution
- Has the desired  $1/q^4$  behavior for  $q^2 \rightarrow \infty$

The charge radii are defined as

$$\langle r_i^2 \rangle = -\frac{6}{dq^2} \left[ \frac{\hat{G}_i(q^2)}{\hat{G}_i(0)} \right]_{q^2=0}$$

$$\langle r_i^2 \rangle = \frac{12}{M_i^2}$$

# Experimental Results

$r_A = 0.80(17)$  fm       $\nu$  scattering

$r_A = 0.74(12)$  fm      Electroproduction

$r_A = 0.68(16)$  fm      Deuterium target

# Extracting Axial form factors

$$\text{Im}(R_{51}) = 4 M_N \left( -\frac{q_1 q_3}{2M_N} \widetilde{G}_P \right)$$

$$\text{Im}(R_{52}) = 4 M_N \left( -\frac{q_1 q_3}{2M_N} \widetilde{G}_P \right)$$

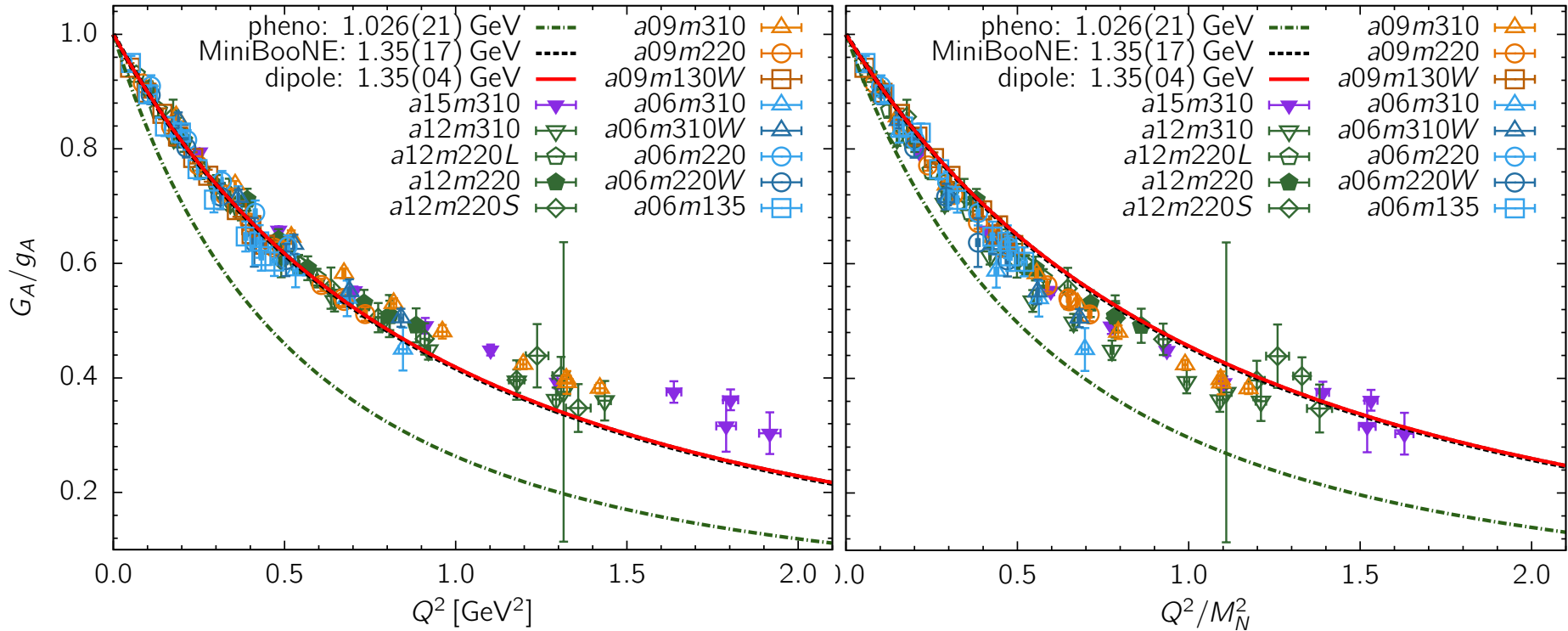
$$\text{Im}(R_{53}) = 4 M_N \left( (M_N + E) G_A - \frac{q_3^2}{2M_N} \widetilde{G}_P \right)$$

$$Re(R_{54}) = 4 M_N q_3 \left( G_A + \frac{M_N - E}{2M_N} \widetilde{G}_P \right)$$

ESC in  $R_{54}$  is large

# Clover-on-HISQ data

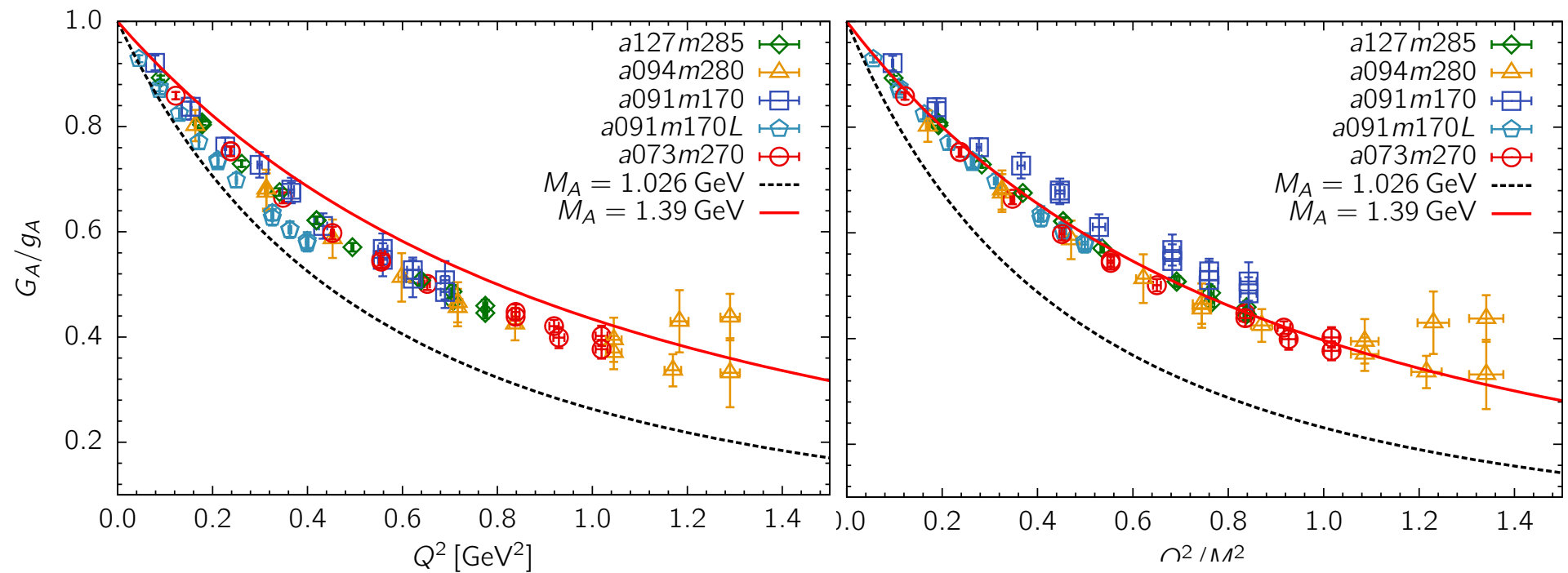
PNDME unpublished



NOTE: The two dipole curves with  $M_A = 1.35$  and  $M_A = 1.026$  are drawn to only provide a reference for the spread and uncertainty in the lattice data

# Clover-on-clover data

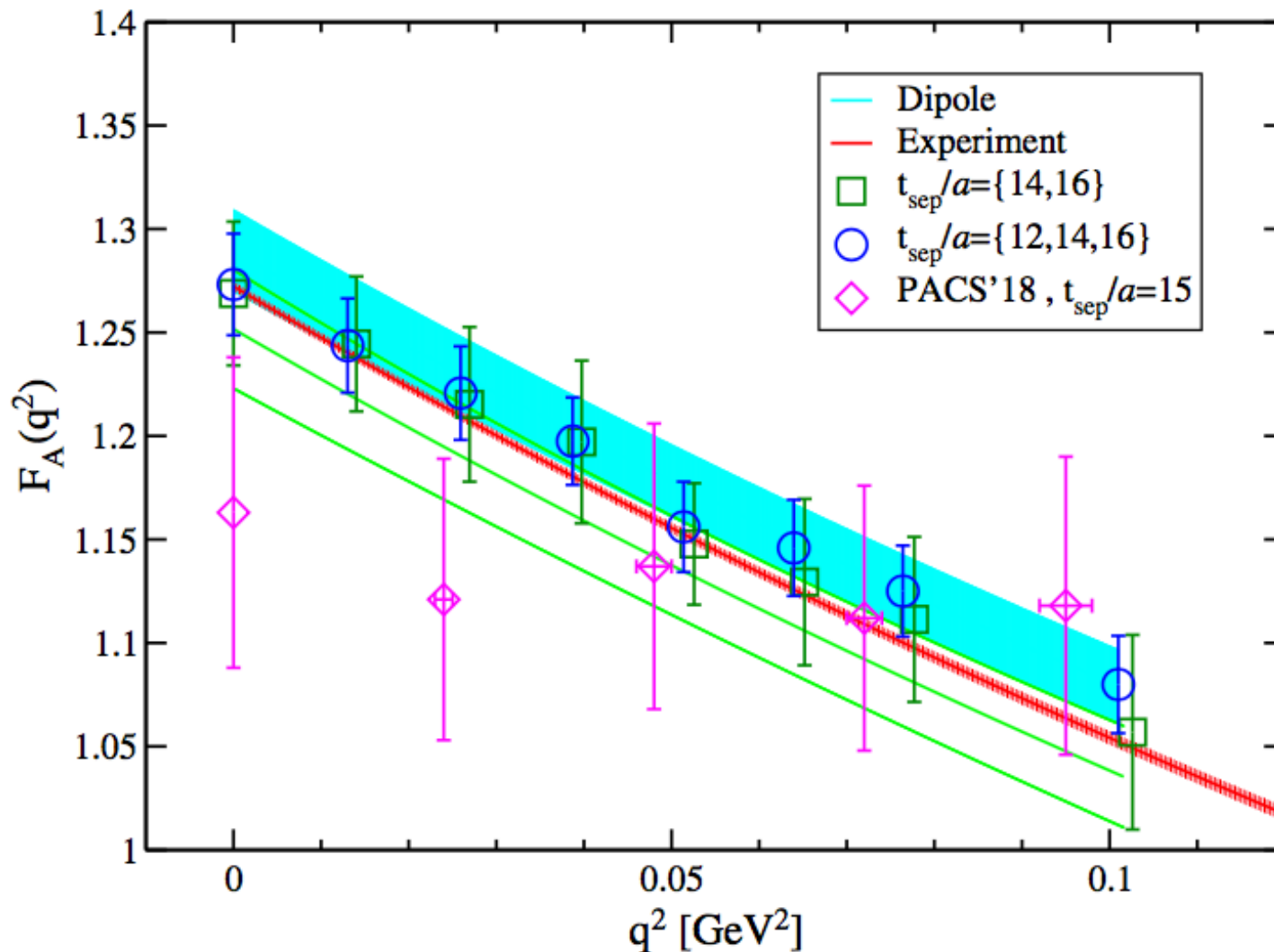
NME unpublished



The statistics of the *a091m170* data (blue squares)  
will be increased by 4X

# PACS: Data at small $Q^2$

PhysRevD.99.014510



# Do $G_A$ , $\widetilde{G}_P$ , $G_P$ satisfy PCAC?

*Brief statement of an unsolved issue*

The operator relation ( $\partial_\mu A_\mu = 2\hat{m}P$ ) holds when inserted in correlation functions in lattice data.

PCAC also implies a relation between form factors

$$2\hat{m}G_P(Q^2) = 2M_N G_A(Q^2) - \frac{Q^2}{2M_N} \tilde{G}_P(Q^2)$$

This is violated.

We have tracked the problem to ME of  
 $\partial_4 A_4 \neq (E - m)A_4$

Since this relation should hold in the ground state, what do large violations at  $t_{sep} \sim 1.5$  fm imply for control over ESC?

# Summary

- Data for isovector charges and form factors becoming precise at the few percent level for  $Q^2 < 1 \text{ GeV}^2$
- Need to understand why the 3 form factors  $\mathbf{G}_A, \widetilde{\mathbf{G}}_p, \mathbf{G}_p$  do not satisfy PCAC
- Lattice values of the charge radii  $r_A$  are smaller than “phenomenological” estimates.
- Are all the systematics under control?
- Need data at smaller  $Q^2$  to improve  $\langle r_i^2 \rangle$  (PACS)
- Disconnected contributions reaching similar maturity